IJESRT

INTERNATIONAL JOURNAL OF ENGINEERING SCIENCES & RESEARCH TECHNOLOGY
FAULT PREDICTION AND ANALYSIS TECHNIQUES OF SOLAR CELLS AND PV MODULES

Dalvir Singh & **Prof. Rupinderjit Singh Kathuria**
M.Tech Scholar, Dept. of Power Engineering, Guru Nanak Dev Engineering College, Ludhiana, India
Associate Professor, Dept. of Electrical Engineering, Guru Nanak Dev Engineering College, Ludhiana, India

ABSTRACT

The photovoltaic market has quickly increasing over a couple of years. One of the main reasons for this high growth in PV industry is the reduction of PV production costs. The output power obtained from the PV module is mainly depend upon the two parameters named as irradiance and temperature. There are number of factors that affects the performance of the PV array, such as diode and connection loss, mismatch loss, DC/AC wring loss, sun tracking loss, shading loss, soiling loss and material loss. From the above mentioned techniques, in the proposed research work, we have considered three faults named as shading loss, soiling loss and material loss. When these faults occur in the network, the power loss of the module decreases. In this research work, we have presented a simulation model fault detection procedure for PV systems, based on the power losses analysis. This automatic supervision system has been developed in MATLAB (MATrix Laboratory) &in Simulink environment. It includes parameter extraction techniques to calculate main PV system parameters for monitoring data in real conditions of work, taking into account the environmental irradiance and module temperature evolution, allowing simulation of the PV system behaviour in real time. The automatic supervision method has analysed the output power losses in the DC side of the PV generator, capture losses. Also, a classification technique named as ANN (Artificial neural network) is used to classify the type of error and to know the level of power loss. ANN is also used to reduce the power loss occurred in the PV array. The performance parameters named as power loss, Idc and Vdc are measured. The power loss is measured without ANN and with ANN to know the efficiency of the system.

Keywords: Dusting and soiling, Shading and material faults, Photovoltaic model, Solar cell.

I. INRTODUCTION

Solar power is considered as the main form of solar energy. Solar energy is transformed into electricity with the use of either indirect method (concentrated solar power) or direct method (photo-voltaic). The large beams of sunlight are determined for small beam by mirrors/lenses for concentrated solar power [1]. The photoelectric effect is utilized by Photovoltaic for converting solar energy into electric energy. Mainly three kinds of faults exist in the solar cell named as Micro Cracks, Snail Tracks, and Hotspot. A detail description of these faults is explained below [2]:

i. Micro Cracks

Micro cracks occurs in solar cell is a normal problem and cannot be avoided [3]. As the name is micro means the output power is affected by a very small crack occurs in the PV panel. The crack may occur due the following reasons:

- Due to the mechanical stress and the shocks occurs during the transportation.
- Due to the aging factor.
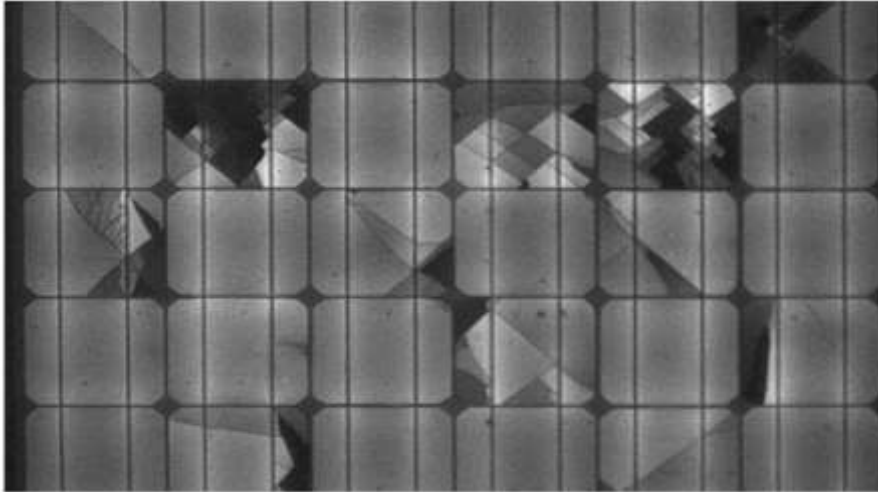- Due to the increase in the temperature

Figure 1: Micro-cracks in a solar PV module

The maximum crack that can be allowed in the single cell of a PV array is defined by the equation below:

$$\frac{B_{inactive}}{B_{Total}} < \frac{I_{\frac{s}{c}} - I_{pmax}}{I_{\frac{s}{c}}}$$

ii.   Snail Tracks

Snail tracks are a product of the formation of silver carbonate (AgZC03) nano-particles which discolor the silver grid. These are usually some discolored lines both on mono and multi crystalline silicon solar modules due to a local discoloration of the Ag contact fingers. So far known, snail tracks occur on the cell edges or close to the Micro Cracks in the Solar PV. These tracks are dependent on material and process induced sources [4].

iii.   Hotspot

This is occurs due to the overheating for a defect known as shunts. This fault takes place along with the normal degradation of material of the solar PV module. During Hotspot, the defected area shows an increased temperature with respect to the remaining cells [5].

II.   PV MODULE FAILURE

The model failure that are occurs in the proposed work comprises of

i.   Dust and soiling

The performance of a solar PV array is mainly depends upon the dusty atmosphere. The performance is changes with the change in position and environment. Numerous experiments are still carried out for the assessment of performance of PV modules due to dust in different region [6]. Although, it is concluded by different researchers, that the performance of the system is decreased by 20% of the efficiency of a solar PV module. The dust loss percentage is measured by the equation written below [7]:

$$Dustloss(\%) = \frac{L_{cc} - L_{DC}}{L_{cc}}$$

Here, L_{cc} represents the irradiance value determined by the clean reference solar cell and L_{Dc} is the irradiance value determined by the dirty reference solar cell

Figure 2: Soiling module

ii. Shading

Shading is a serious problem in PV systems. It can cause a significant decrease in performance and may damage the arrays. When a cell is shaded, its current is lower than it would normally be [8]. Although some types of shading are unavoidable, like the shading produced by the clouds, some can be prevented but are often overlooked, such as the presence of trees that could grow tall enough to obscure the solar panels. If the system is being installed during summer months when the sun's trajectory is at its highest, sometimes installers may not account for the fact that during other months when the sun's trajectory is different, the trees or other buildings may get in the way between the solar panels and the sunlight's trajectory, as shown in figure below [9]
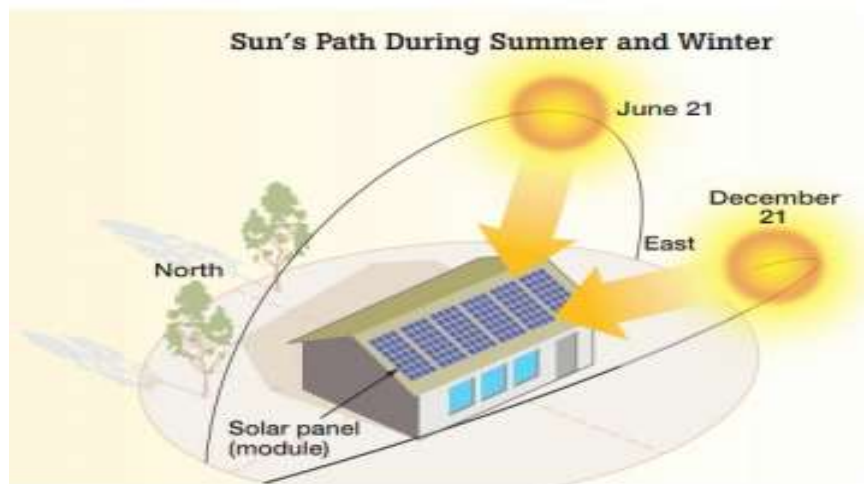
Figure 3: Surrounding vegetation may keep the sunlight from reaching the solar panels during some months, but not in others

iii. Packaging material faults

Module package degradation is a major problem, which results in poor module performance and a safety hazard. Even though, it is often overlooked because package degradation is very slow and hard to detect [10]. The package material faults occur due to the aging of the module, hot spot, moisture occurs in the system. Package damage can produce safety hazards in high voltage systems due to the lack of protective insulation. Such failures may induce electric shock and create a pathway for electrochemical corrosion. The potential shock hazard can be worsened by moisture intrusion into the package. Some typical module package degradations include glass breakage, encapsulate discoloration and delaminating [11].

These days' production of electricity in the world is mainly fossil fuel based. Eco-friendly power generation is a burning issue for power generation. Solar Energy solves this problem very well [12]. Scientists are trying to increase the efficiency of Solar PV modules to use them more efficiently as an alternate source of fossil fuel for power generation. But; efficiency of Solar PV Cells and Modules can reduce due to faults generated inside of them. Thus, to detect these faults immediately and to know the current & voltage loss in the PV system is also become a problem [13]. These faults may occur due to wide range of reasons such as due to micro cracks, snail tracks and hotspot in the PV system. This problem has been approached by developing a new method based on similarity measures within a single installation. A limitation of this method is that only a single panel fault can be detected at each point in time. The issue is how to solve these problems efficiently in the presence of different system configurations, with geographic and thermal dependencies as all system delivers different power curves. The implemented method solves the problem by locating similar time periods. This is followed by calculating the degradation ratio in both voltage and current samples respectively.

III.   RELATED WORK

L. Wang et al. (28, 2017) proposed an online algorithm to diagnose faults of PV module based on multi-class support vector machine (SVM). The simulation models of the photovoltaic module have been implemented and the output power generation characteristics of PV modules under two typical fault conditions (line-to-line fault and abnormal degradation fault) have been analyzed. **Ali et al. (22, 2017)** proposed a techniquefor real time monitoring and fault diagnosis in photovoltaic systems. The proposed method has been based on a comparison between the performances of a faulty photovoltaic module, with its accurate model by quantifying the specific differential residue that will be associated with it. **Dhimish et al. (29, 2017)** presented a new algorithm for detecting faults in grid-connected photovoltaic (GCPV) plant. There are few instances of statistical tools being deployed in the analysis of photovoltaic (PV) measured data. The main focus of this research is to outline a PV fault detection algorithm that can diagnose faults on the DC side of the examined GCPV system based on the t-test statistical analysis method. **Kashyap et al. (30, 2017)** proposed a novel scheme for the fault detection in a DC-DC converter connected to a solar PV module with the help of a proposed state machine based model. This scheme can be practically employed by applying Peak Current Mode (PCM) control technique with an excessive ramp signal. **Karim et al. (31, 2015)** analyzed and determine the reduction of efficiency for faults associated with Solar PV cell and modules. Also, different fault detection scheme are discussed that are adopted worldwide. The main focus is concentrated in various faults that hinder the power generation of PV modules. The faults of PV cell and modules have been discussed. The aim of this paper is to quantify the loss of production and efficiency as well as to assume the fault level approximately by mathematical modelling if a fault starts to develop. The different standard PV module testing procedures have been discussed.

IV.   SIMULATION MODEL

This research has analyzed the fault detection in PV module. Power loss is measured due to three kinds of faults such as dusting and soiling, shading and material faults. The flow by which the methodology of work takes place is shown in figure below:

Step1: Design a simulator for fault detection and analysis in PV array.

Step2: Create an array of PV which is known as PV array using PV module.

Step3: Design an inverter to control the output of a PV array.

Step4: Initialize the ANN within the simulator to analyze and detect the fault due to the dust, soiling and material fault.

Step5: After the detection of fault we analyze the effects of fault.

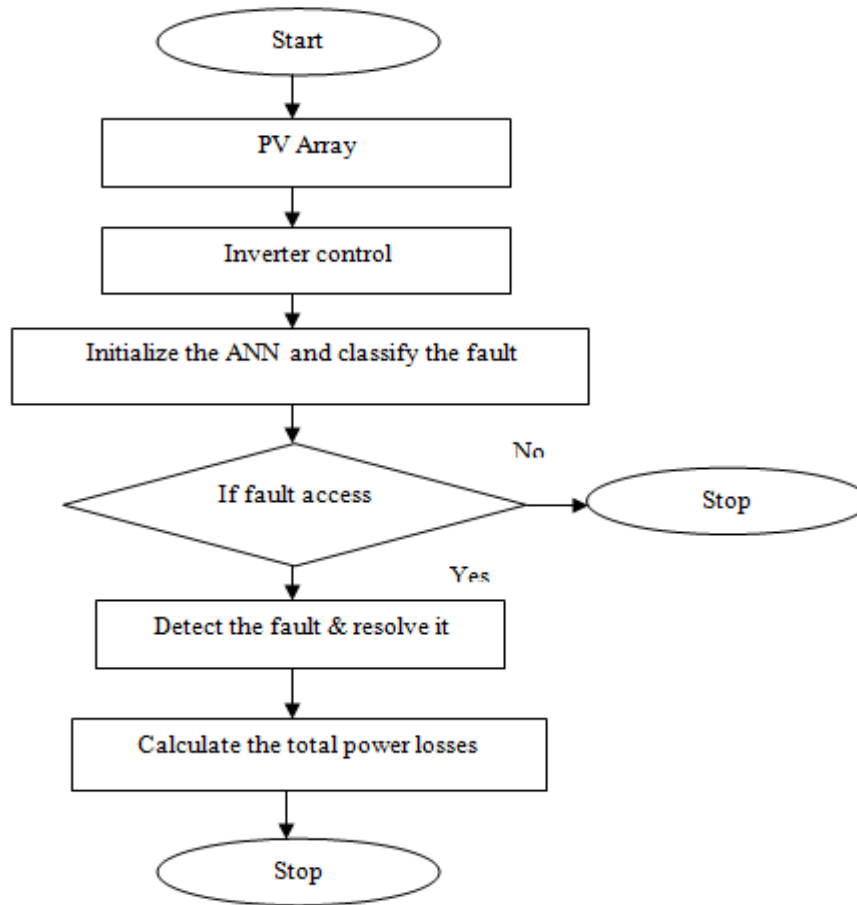Step6: To analyze the simulation model we calculate the performance parameters of proposed work.

Figure 4: Proposed workflow

V. RESULT AND ANALYSIS

The dataset is taken from the Econergy - A California corporation (1 MW Solar plant) V.P.O. Boparai kalan, Distt. Ludhiana.

*Table 1: Temperature observed on May Month*

Time	Date	Temperature (°C)
07:00 am	01/05/2018	21
08:00 am	01/05/2018	24
09:00 am	01/05/2018	25
10.00 am	01/05/2018	27
11.00 am	01/05/2018	31
12.00 pm	01/05/2018	38
01.00 pm	01/05/2018	43
02.00 pm	01/05/2018	44
03.00 pm	01/05/2018	43
04.00 pm	01/05/2018	42
05.00 pm	01/05/2018	41
06.00 pm	01/05/2018	37
07.00 pm	01/05/2018	36

Above figure represents the temperature on the month of May in Econergy - A California corporation (1 MW Solar plant) V.P.O. Boparai kalan, Distt. Ludhiana. The sample for three different faults named as soiling module, shading module and cracking module are shown below are tested on this database

*Figure 5: A sample of soiling appear in PV array*
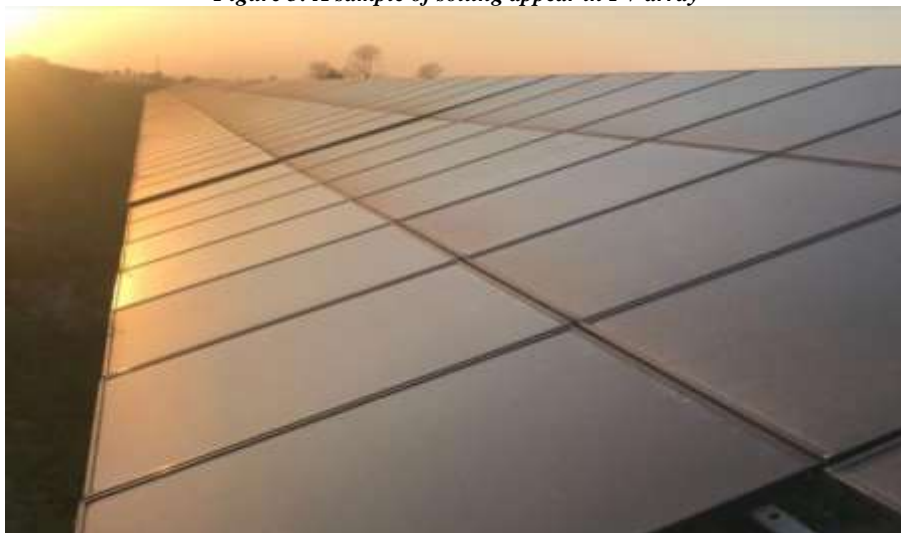
Figure 6: A sample of fading appear in PV array

Figure 7: A sample of crack appear in PV array

Title window of MATLAB is shown in figure 8.In this window the title of the proposed model has been displayed as the title of our research work is "Fault Analysis and Detection Techniques of Solar Cells and PV Modules based on artificial intelligence technique"
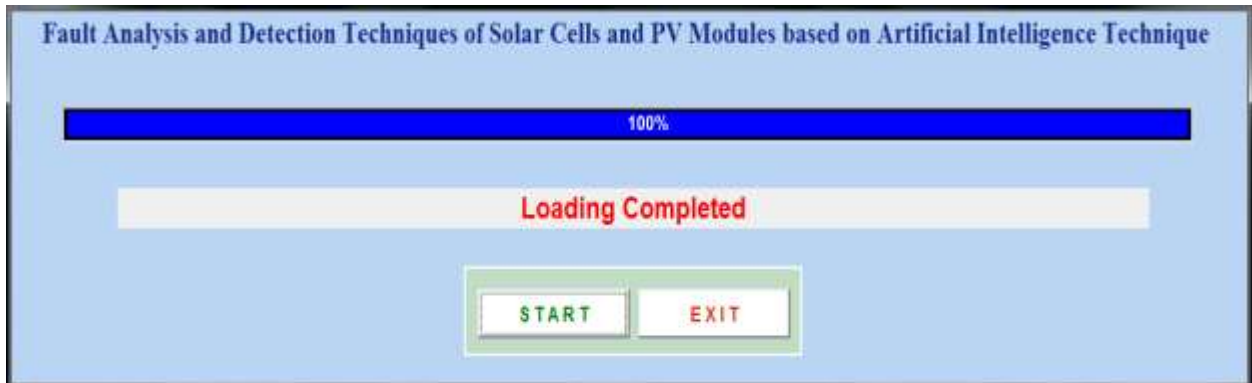
Figure 8: Title window

This title has been displayed below. Title window also contains two options which are start and exit. If we click on start, simulation window opens and if we click on Exit, the simulation window closed
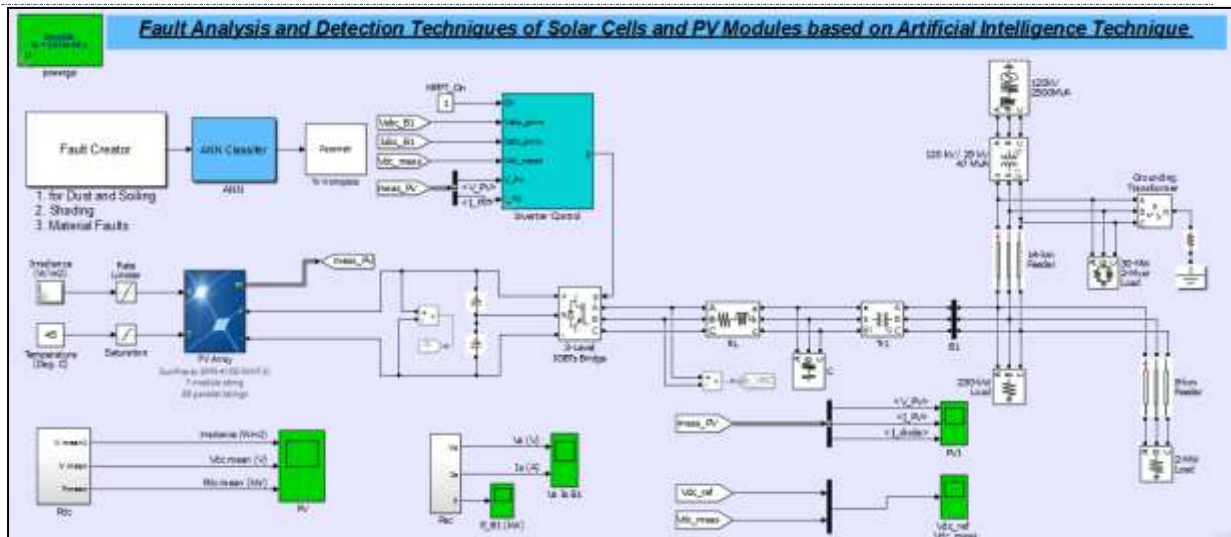
Figure 9: Simulation model

The above figure is the main simulation model of the proposed work. The above model displays after the completion of processing. The model has two inputs such as temperature and irradiance. The temperature is measured in degree Celsius and irradiance is measured in W/m^2. Irradiance input is applied to the PV array through rate limiter whereas temperature is applied to the PV array through the saturation. The output of the array is the output power that is used to generate electricity and can be used as an input to the tube light, fan, TV etc. The PV array generates three outputs one is named as meas_PV and other two becomes the input to the 3 level IGBT's bridge. The +ve output of PV array is connected to the +ve terminal of the IGBT and the -ve output of PV array is connected to the -ve input of the IGBT bridge. The third input to the IGBT bridge is Neutral connected between the battery point. Here in IGBT Bridge the diode is used to the neutral point to neutralize the load.

The research is mainly to observe the effect of faults occur in the PV array system. In the proposed work, mainly three faults are created named as the fault occurs due to dust and soiling, shading, and material faults. Here after creating the three faults mentioned above, ANN is used as a classifier to know which fault is appear in the PV array. After detecting the fault the parameters named as Vabc_B1, Iabc_B1,Vdc_meas and meas_PV. Here ANN is used to know the power loss occur in the PV array by measuring the power level.

The output generated by the PV array meas_PV is provided as an input to the inverter controller that comprises of voltage and current. The output of inverter becomes the input to the 3-level IGBT Bridge. The output of IGBT bridge is connected to different loads named as RL (resistor inductor) load, capacitor load, transformer load, parallel load etc.
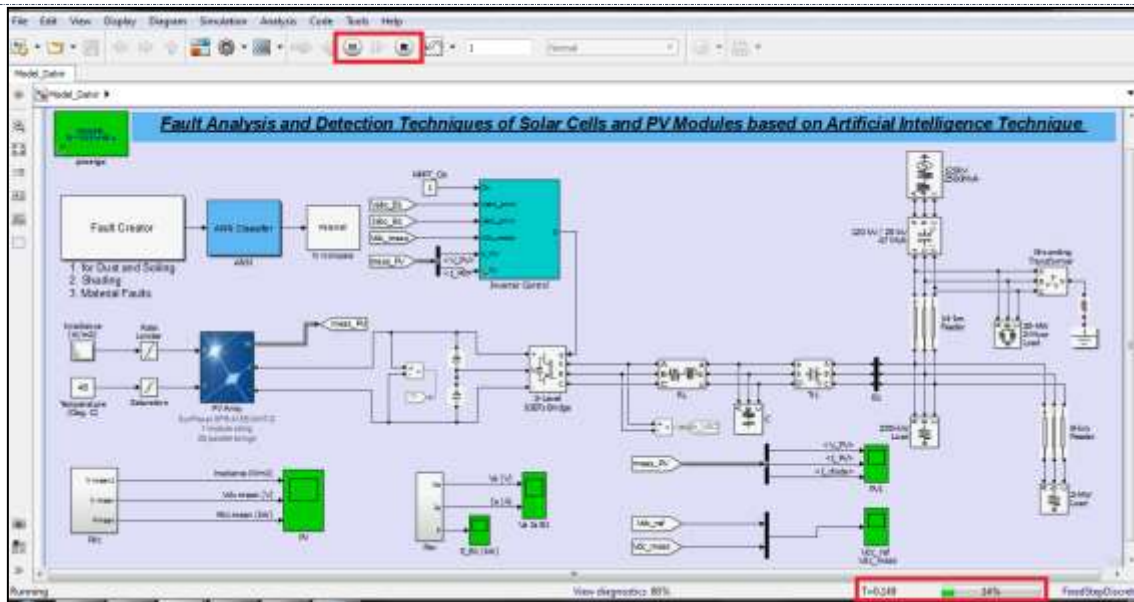
Figure 10: Running model

The above figure represents the running model of the proposed work. Here the red block at the top of the model represents that the model is in its running state and the time set for the simulation is 1 minute. The processing is shown inside the red box for time T=0.149 minute the processing is 31 %. Here the green box represents that when we click on PV scope the waveform measured for Irradiance, Vdc and Pdc are displays on the screen.
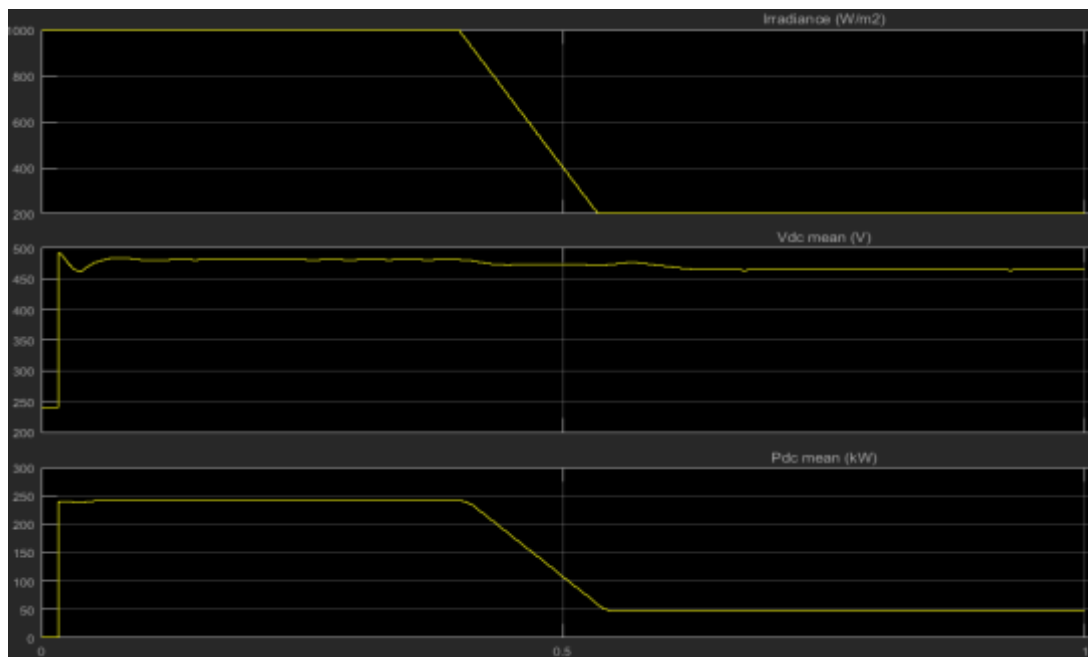

Figure 11: Irradiance, DC Voltage and DC Power

The above figure represents the waveform obtained for irradiance, Vdc, and Pdc. When we click on PV scope, above waveform displays on the screen. The above waveform represents the graph between irradiance, Vdc, and Pdc with respect to time. Irradiance as an input provided to the PV array is represented in the waveform. The maximum value of irradiance provided to the PV array is 1000 w/m^2. Here, Vdc mean represents the DC voltage generated by the PV array system and having a maximum value generated by the system is 500. Pdc waveform represents the power generated by the system. The maximum power generated is 250 KW whereas minimum power generated is 50KW obtained after 0.5ms
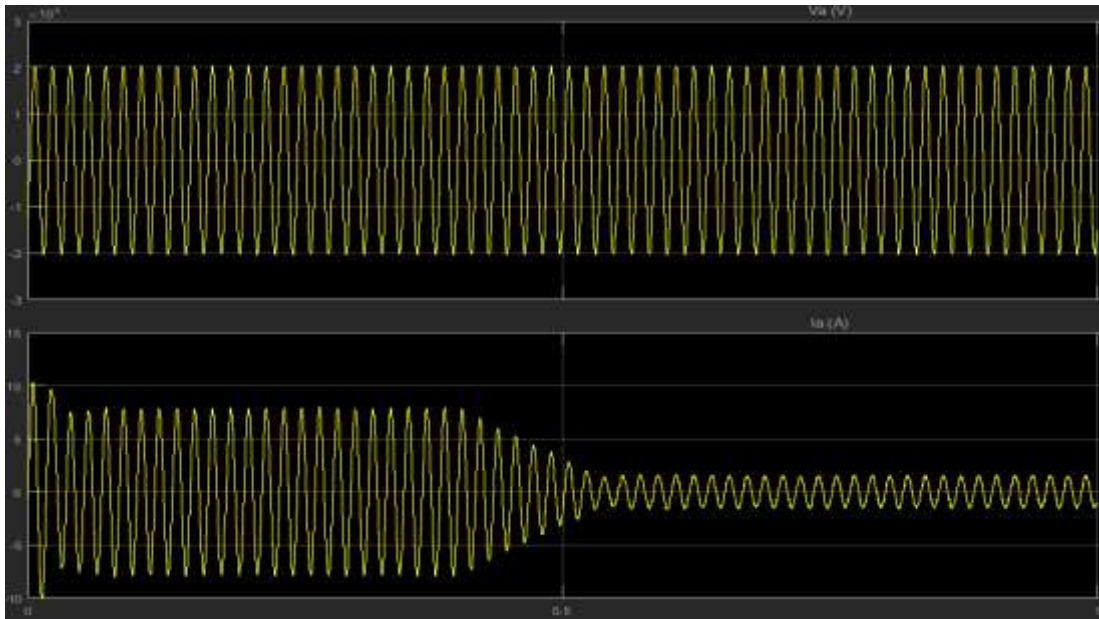
Figure 12: AC Voltage and Current

The above waveform represents the ac voltage and ac current obtained by using inverter. The power generated by the PV cell is stored in DC voltage. Thus to stored their energy battery is used. To use generated power as an input to the electrical equipments connected in the house the dc power is converted into AC power. The representation of voltage and current is shown above. The maximum amplitude of voltage is 2volt whereas maximum amplitude of current is 10A. After 0.5 time current is reduces as shown in figure above.
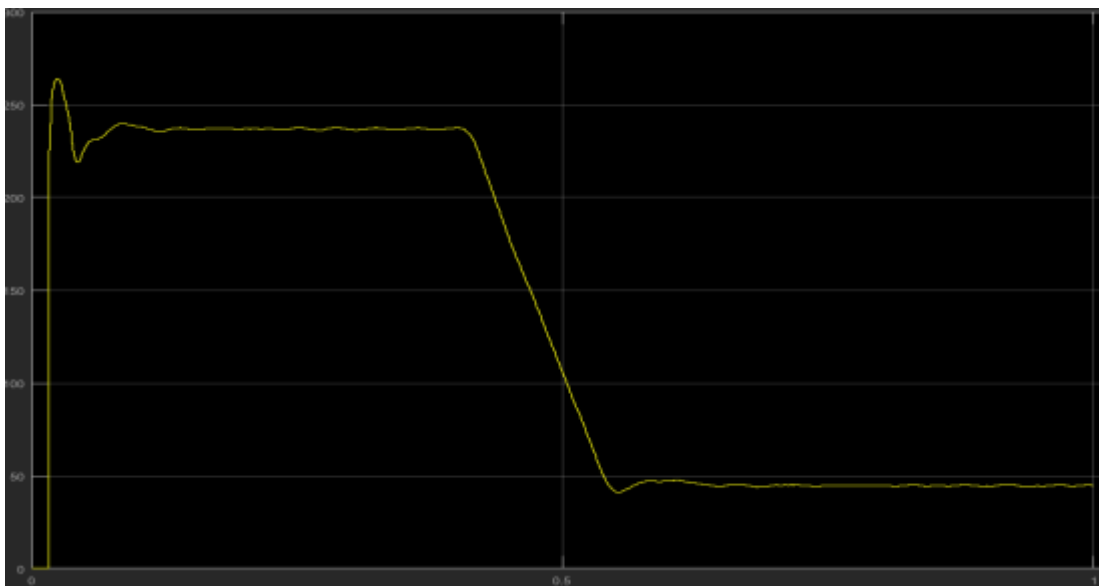
Figure 13: AC Power

The above figure represents the AC power generated by the inverter. The output of PV array is DC which is provided as an input to the inverter that converts DC power into AC power. The voltage level generated by the PV array is nearly 260 volts. The voltage decreased after 0.5 m and become 50 V.
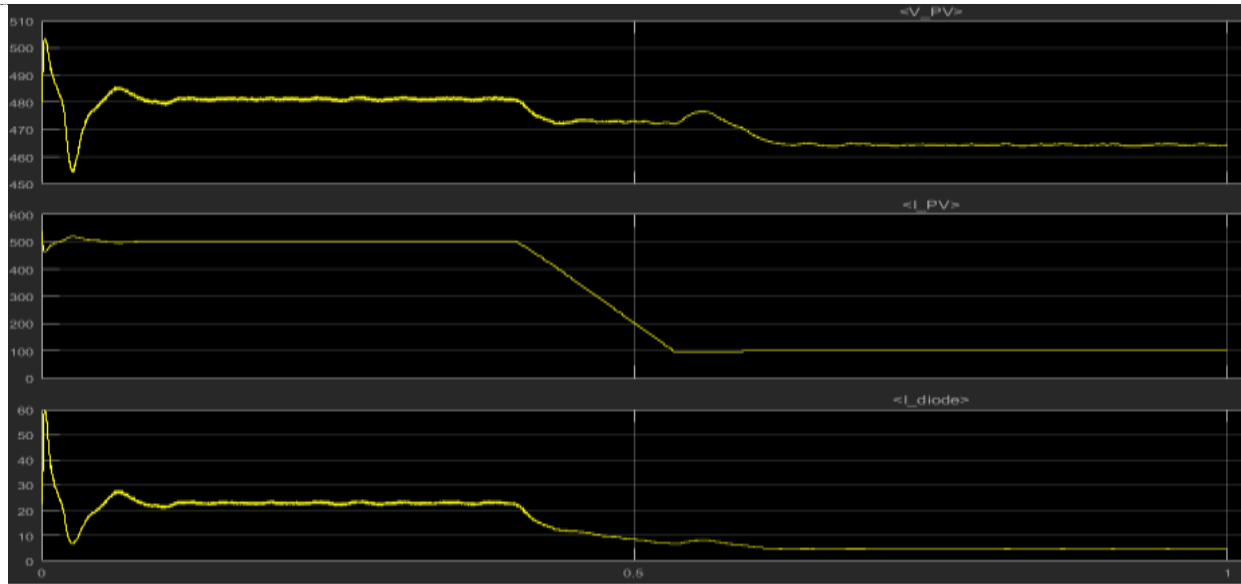
Figure 14: PV Voltage, PV Current and Diode Current

The above figure represents the individual voltage, current generated by single PV cell. The maximum value of voltage is 500V whereas minimum voltage generated is460V. The maximum current generated by the single cell is 500A. As the time increases the PV current as well as the diode current reduced. The minimum value of PV current is 100 A and the minimum value of diode current is 5A.
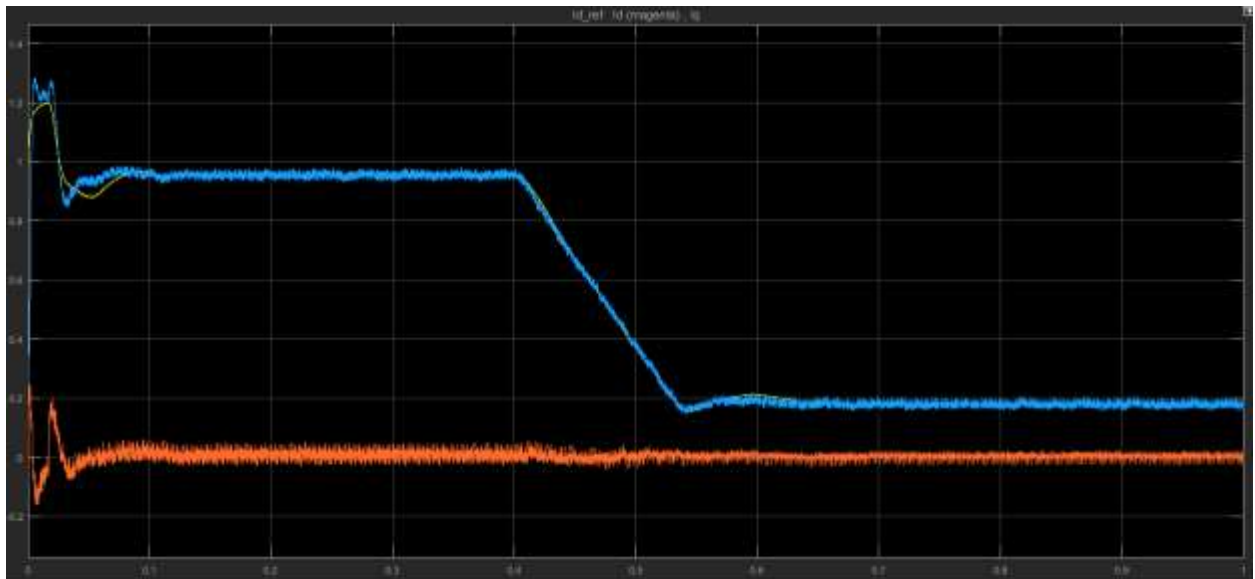

Figure 15: Id_reference, Id (Magenta) and Iq

The above figure represents the three waveforms Yellow line represents the Id_reference, blue line represents the Id (Magenta) and orange line represents the Iq current. It is clear from the figure that Td reference and Id (magenta) line are overlapping to each other. The Iq current is less having maximum amplitude of 0.2 A.
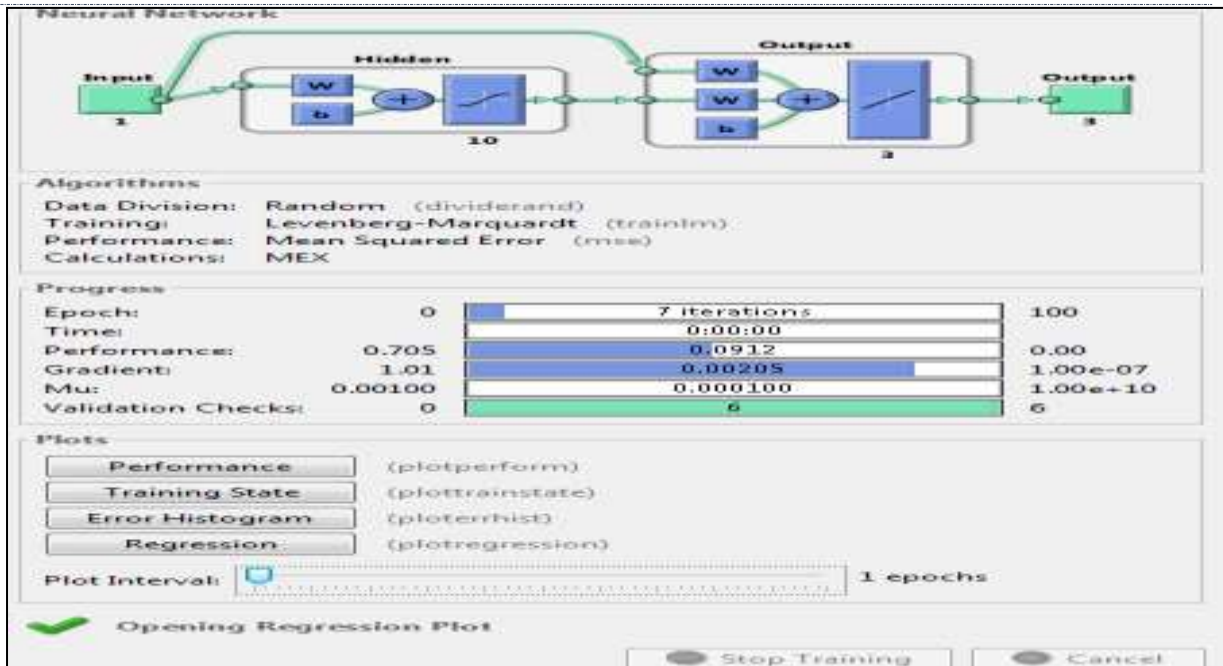
Figure 16: ANN Structure

The above figure shows the structure of artificial neural network used in the proposed work. Neural network mainly used three network layers named as input hidden and output layer. The input is given to the hidden layer, which comprises of weight W and b is the bias. The weight of the neurons is adjusted in such a manner that the desired output is obtained. The weight of the undesired output of neural network is adjusted by using bias. Bias is a very small value that is added to the undesired output so that it can be adjusted to the desired category. Here there is one input, 3 is the number of output with 10 numbers of hidden neurons. The progress of the neural network is observed by using the variables defined below. These variables are named as epoch, time, performance, gradient, mutation and validation check. When any of this parameter is satisfied, the desired output is obtained. When the validation check is completed, the desired output is obtained
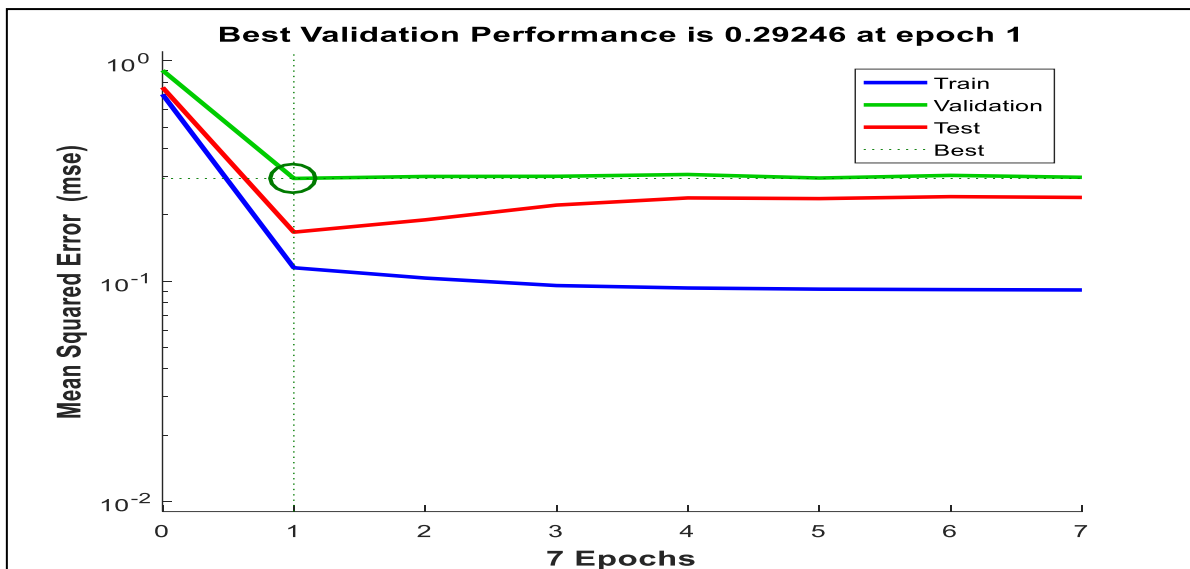

Figure 17: ANN Performance evaluation (MSE)

The above figure represents the mean square error of the neural network. The MSE is measured with respect to the number of epoch. The MSE is measured for training, validation, testing and best. The value of MSE

observed in the proposed work is less than zero which means that neural network performs well in order to know the type of fault occurs in the PV array and to reduce the fault.
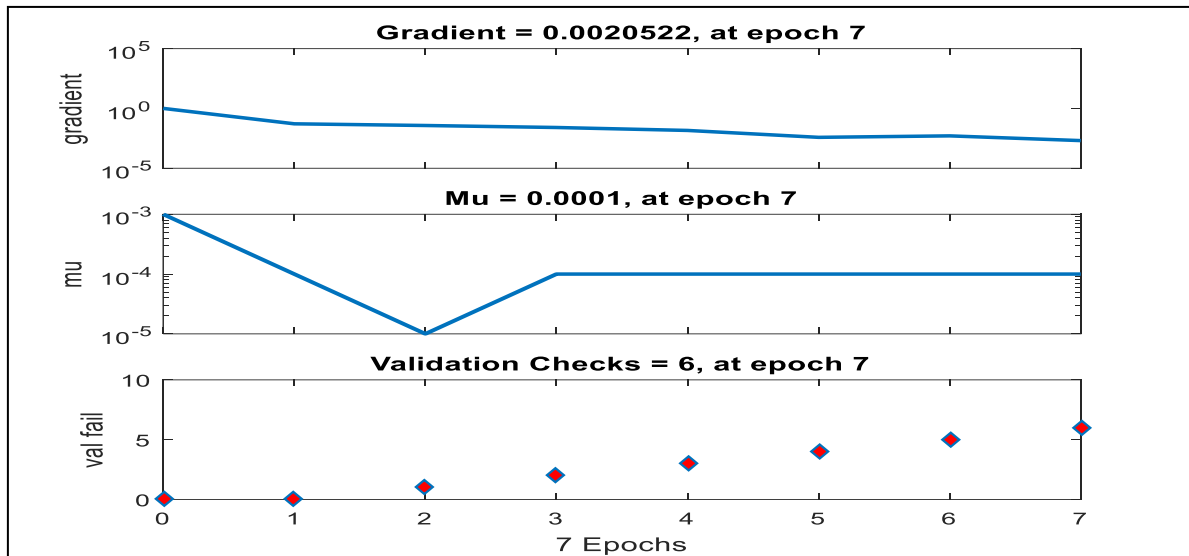

Figure 18: ANN Parameters

The above figure represents the parameter values of ANN such as gradient, mutation and validation fail. The gradient value represents the input provided to the neural network. Here the best input value of gradient is 0.0020522 which is obtained at 7th iteration. For this gradient value neural network add mutation value that is also known as bias value to adjust the input value in such a manner to obtain the desired output. Here the value of mutation added to the gradient is 0.0001. For gradient and mutation values the validation check is 6. The neural check mainly checks the same data maximum up to 6 validations.
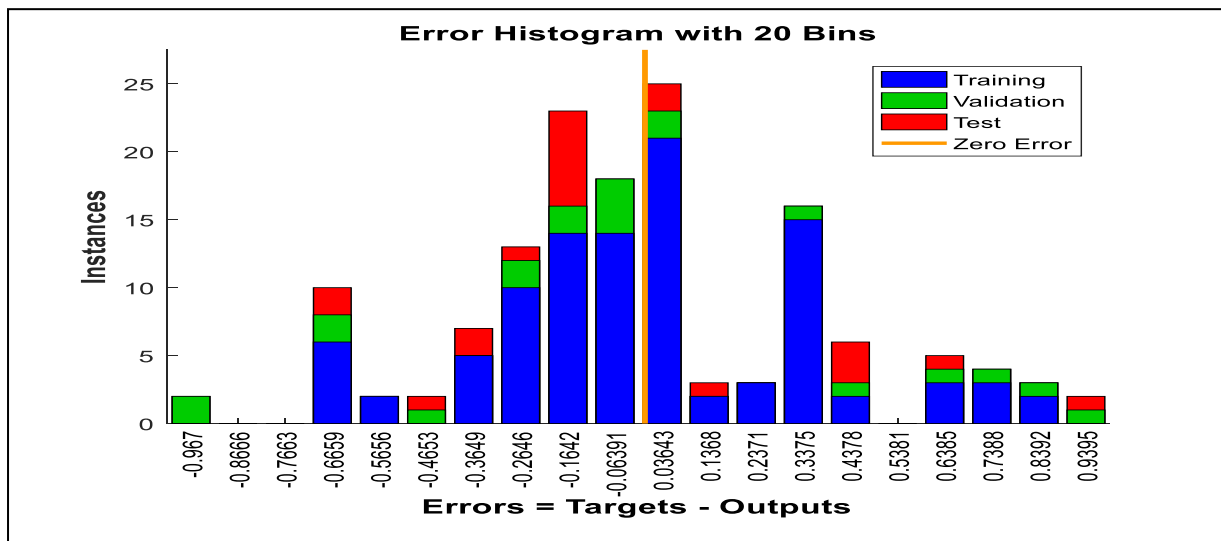

Figure 19: ANN Error Rate

The above figure represents the histogram graph for the error rate of artificial neural network. The above figure comprises of three types of data named as training data, validation data and test data represented by blue color, green color and red color. The orange color represents the zero error. From the above figure it is clear that the training data is large as compared to test data and validation data.
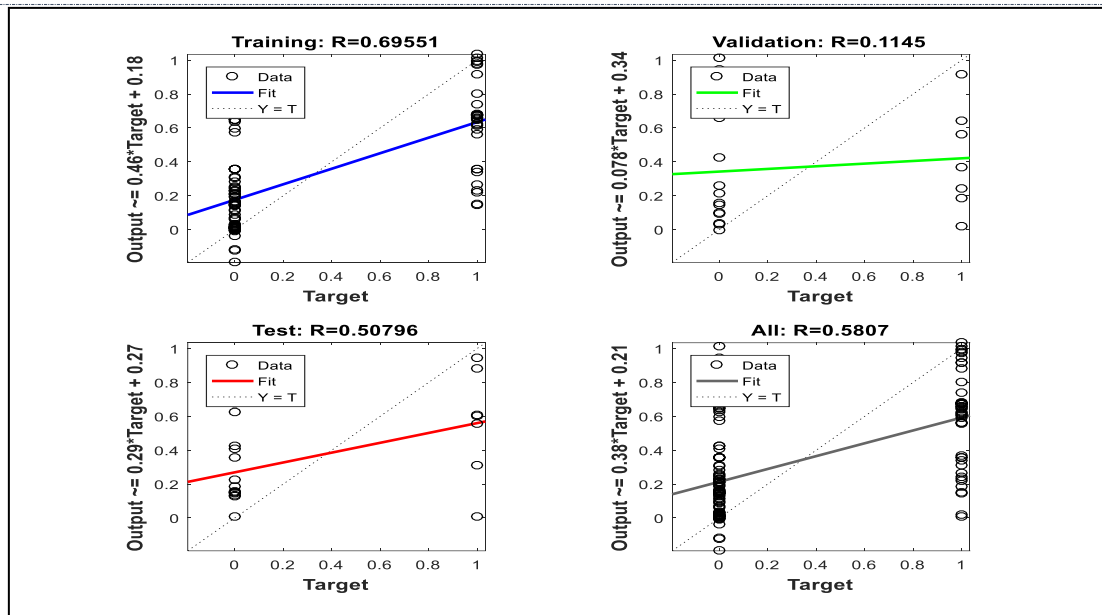
Figure 20: ANN Regression Plot

The above figure represents the four graphs for training validation, testing and regression. From the above figure it is clear that when the training data is 0.69551, testing data is 0.50796 and validation value is 0.1145 the regression value obtained is 0.5807. The regression value represents the output measured by integrating training, testing and validation values.
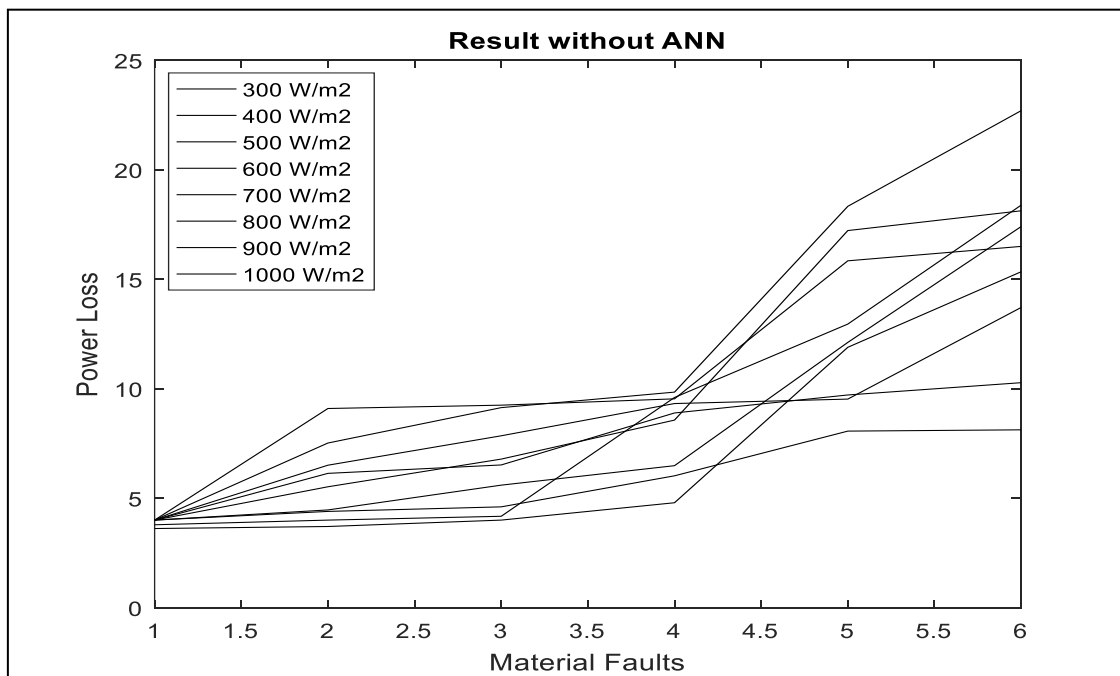

Figure 21: Power loss without ANN

The above figure represents the power loss measured by the simulator when neural network is not used. The power loss is measured for the material fault. The material faults occur due to the aging of the module, hot spot, moisture occurs in the system. X-axis represents the number of material faults appear in the PV array and Y-axis represents the power loss. The maximum power loss observed for the PV array is nearly 23 KW.
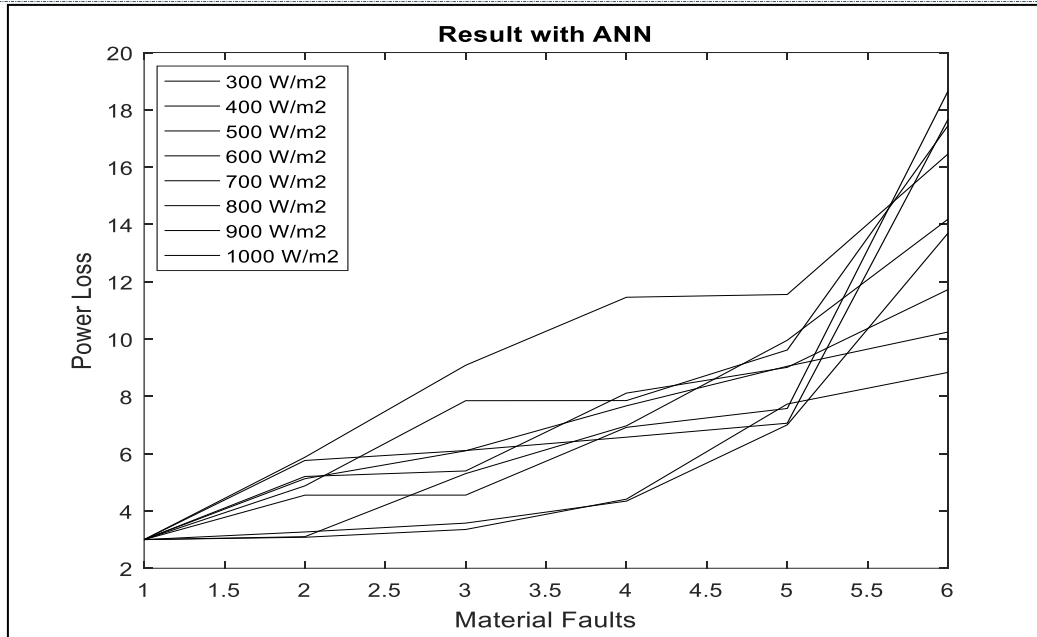
Figure 22: Power loss with ANN

The above figure represent the power loss measured for material fault occur in PV array when ANN classifier is applied. From the above figure it is clear that the power loss is reduced from 23 KW to 18 KW when ANN is applied in the simulation model. This is done by excluding the fault area of the PV array ad considering the accurate area. This helps to reduce the power loss of PV array. The comparative analysis of proposed work is given in below section with tabular form.

Table 2: Comparative analysis of Power Losses

S. No.	Time (HH:SS)	Temperature (°C)	Power Losses with ANN	Power Losses without ANN
1	10:00 am	27	18.3	23.6
2	12:00 pm	38	12.2	18.9
3	02:00 pm	44	9.6	15.7
4	04:00 pm	42	10.4	14.4
5	06:00 pm	37	16.7	18.3

Above table represents the comparative analysis of proposed work with artificial neural network and without artificial neural network. From the observation, it is clear that the power losses are less in case of artificial neural network at the same temperature. The maximum power losses is 23.6 and it is occurs when we simulate our proposed work without artificial neural network. For the same data, when we use artificial neural network then it is 18.3

VI.   CONCLUSION

This research work has presented a fault detection process for PV array systems based on power loss. The SIMULINK & MATLAB tool has been used for the designing of the model and hence; parameters such as voltage, current, and power loss are measured for different faults. The environmental irradiance and module temperature evolution are taken as input in the simulation model. The power losses are analysed in the DC side of the PV generator along with power losses. The power losses are measured for three kinds of faults occurs in the system such as effect of dust and soiling, effect of shading and effect of material faults. The main idea of the proposed system diagnosis and fault detection of a PV system is based in the continuous check of the measured capture losses. For this purpose, we have established theoretical boundaries in which the measured capture losses do not exceed any of them else the system would be considered as faulty. Artificial neural network has been applied in the proposed simulation model that has performed mainly three functions (1) classification of type of fault occur in the PV module (2) determining the power loss level and (3) reducing the power loss by excluding the faulty area of the PV module.

REFERENCES

[1] Ali, M. H., Rabhi, A., El Hajjaji, A., & Tina, G. M. (2017). Real Time Fault Detection in Photovoltaic Systems. *Energy Procedia*, *111*, 914-923.

[2] L. Wang, J. Liu, X. Guo, Q. Yang and W. Yan, "Online fault diagnosis of photovoltaic modules based on multi-class support vector machine," *2017 Chinese Automation Congress (CAC)*, Jinan, China, 2017, pp. 4569-4574.

[3] Dhimish, M., Holmes, V., Mehrdadi, B., & Dales, M. (2017). Simultaneous fault detection algorithm for grid-connected photovoltaic plants. *IET Renewable Power Generation*, *11*(12), 1565-1575.

[4] Kashyap, N., & Gautam, A. (2017, March). Fault tolerant peak current mode controlled flyback converter for solar PV modules. In *Power and Embedded Drive Control (ICPEDC), 2017 International Conference on* (pp. 265-269). IEEE.

[5] Karim, I. A. (2015, May). Fault analysis and detection techniques of solar cells and PV modules. In *Electrical Engineering and Information Communication Technology (ICEEICT), 2015 International Conference on* (pp. 1-4). IEEE.

[6] Patel, H., & Agarwal, V. (2008). MATLAB-based modeling to study the effects of partial shading on PV array characteristics. *IEEE transactions on energy conversion*, *23*(1), 302-310.

[7] Naumann, V., Lausch, D., Hähnel, A., Bauer, J., Breitenstein, O., Graff, A., ... & Hagendorf, C. (2014). Explanation of potential-induced degradation of the shunting type by Na decoration of stacking faults in Si solar cells. *Solar Energy Materials and Solar Cells*, *120*, 383-389.

[8] Tsai, D. M., Chang, C. C., & Chao, S. M. (2010). Micro-crack inspection in heterogeneously textured solar wafers using anisotropic diffusion. *Image and Vision Computing*, *28*(3), 491-501.

[9] Köntges, M., Kunze, I., Kajari-Schröder, S., Breitenmoser, X., & Bjørneklett, B. (2011). The risk of power loss in crystalline silicon based photovoltaic modules due to micro-cracks. *Solar Energy Materials and Solar Cells*, *95*(4), 1131-1137.

[10] Richter, S., Werner, M., Swatek, S., & Hagendorf, C. (2012, September). Understanding the snail trail effect in silicon solar modules on microstructural scale. In *27th European Photovoltaic Solar Energy Conference and Exhibition, EU PVSEC, Frankfurt, Germany* (pp. 3439-3441).

[11] Simon, M., & Meyer, E. L. (2010). Detection and analysis of hot-spot formation in solar cells. *Solar Energy Materials and Solar Cells*, *94*(2), 106-113.

[12] Mani, M., & Pillai, R. (2010). Impact of dust on solar photovoltaic (PV) performance: Research status, challenges and recommendations. *Renewable and Sustainable Energy Reviews*, *14*(9), 3124-3131.

[13] Appels, R., Lefevre, B., Herteleer, B., Goverde, H., Beerten, A., Paesen, R., ... & Poortmans, J. (2013). Effect of soiling on photovoltaic modules. *Solar energy*, *96*, 283-291.

[14] Ramabadran, R., & Mathur, B. (2009). Effect of shading on series and parallel connected solar PV modules. *Modern Applied Science*, *3*(10), 32.

[15] Jorgensen, G. J., Terwilliger, K. M., DelCueto, J. A., Glick, S. H., Kempe, M. D., Pankow, J. W., ... & McMahon, T. J. (2006). Moisture transport, adhesion, and corrosion protection of PV module packaging materials. *Solar Energy Materials and Solar Cells*, *90*(16), 2739-2775.

CITE AN ARTICLE